

# RF BiST to detect IQ Imbalances considering Crosstalk Effects for Advanced Antenna System

KISHORE KHED

MASTER'S THESIS

DEPARTMENT OF ELECTRICAL AND INFORMATION TECHNOLOGY

FACULTY OF ENGINEERING | LTH | LUND UNIVERSITY



# RF BiST to detect IQ Imbalances considering Crosstalk Effects for Advanced Antenna System

Kishore Khed  
ki7132kh-s@student.lu.se

Department of Electrical and Information Technology  
LTH, Lund University  
SE-221 00 Lund, Sweden

Supervisors: Erik Larsson (LTH, Lund University)  
Raihan Rafique (Ericsson AB)

Examiner: Pietro Andreani

November 27, 2018

© 2018  
Printed in Sweden  
Tryckeriet i E-huset, Lund

---

# Abstract

---

Internet of Things (IoT) is a network constituted by uniquely identifiable commodity objects or devices equipped with some sensing system. To achieve high data rates required for IoT devices, a modern wireless communication system, known as Advanced Antenna Systems(AAS), leads to significant improvement, by increasing not only the data rate but also spectrum efficiency and the channel capacity. A certain type of analog signal distortions, i.e. the in-phase (I) and quadrature-phase(Q) imbalances can severely damage the performance of the Radio Frequency (RF) transceivers. The IQ imbalances refer to gain mismatch, phase mismatch, DC offset in the I and Q branches. IQ Imbalances affect the efficiency and performance of the RF Transceivers, present in the AAS. Hence a need for test architectures arises. In this thesis an existing BiST circuitry for one transmission chain is implemented and further extended to multiple transmission chains(up to 4). As the number of transmission chains increase, mutual coupling phenomenon leading to crosstalk effects are to be considered. Along with the designed test signal, the BiST circuitry enables us to detect the transmitter impairment with low computational complexity.

We have considered 3 different cases, that have been implemented. They are - one antenna setup, 2x1 antenna array setup and 4x1 antenna array setup. The first case has one transmission chain. We have utilized the Generalized Memory Polynomial(GMP) power amplifier model, and the existing BiST technique, called as Self-Mixing Envelope Detector method is implemented in Matlab. In the case of 2x1 Antenna array, implementation is partly carried out using the RF equipment for the signal generation stage, power amplifier stage, crosstalk effects( due to mutual coupling), and BiST circuitry stage, was previously implemented in Matlab is utilized. The 4x1 antenna array setup, just like the one antenna setup, is entirely implemented in Matlab. Additionally, the coupling coefficients are extracted to model the mutual coupling phenomenon. In the one antenna setup & the 4x1 antenna array setup, the RMSE% of IQ imbalances are calculated. In the 2x1 antenna array setup, gain mismatch, phase mismatch, both the DC offsets are measured up to a certain accuracy.

The results obtained in all the three cases advocate that this method, successfully detect the IQ impairments present in the advanced antenna system, even when the crosstalk effects are considered.



---

## Popular Science Summary

---

*Internet of Things (IoT)* is network constituted by day-to-day objects equipped with some sensing system. These objects can also communicate with other objects for data exchange, wirelessly. This calls for a need of better wireless communication systems. New techniques using the 4G (Long-Term Evolution) have been developed to solve this problem, known as Advanced Antenna System (AAS). This new technique include packing a large number of antennas in a small area, enabling the transmission of signals of the same frequency, at the same time. Closely packing the antennas, causes a phenomenon called as mutual coupling leading to crosstalk effects in the Radio Frequency(RF) system. Effect on an antenna due to the adjacent antenna is called mutual coupling and it leads to crosstalk effects. Due to the crosstalk effects the functioning of the antenna changes.

AAS consists of multiple RF transmission chains, each transmission chain is made of an in-phase (I) and a quadrature-phase (Q) branch. In reality, there is always some imbalances present between I and Q branches of the RF transceivers. The I & Q imbalances can severely damage the performance of RF transceivers. These occur due to finite tolerances of the hardware components used in the RF transceivers. These spurious effects are mainly due to amplitude & phase mismatches, and dc offsets between respective IQ branches and therefore known as IQ imbalances. These IQ imbalances are one of the most detrimental imperfections in the performance of an RF transceivers. Hence a need for a test architecture arises.

Testing a circuit requires the application of a test stimulus and the comparison of the actual circuit response with the correct response. If the system internally does this process and gives us a result which enables us to determine if the system is faulty or not, then it is referred to as a Built-In Self Test method of testing, commonly abbreviated as *BiST*. When this technique of testing is applied to an RF system, it is called RF BiST.

In this thesis, using an RF BiST method, we detect the IQ imbalances, considering crosstalk effects for Advanced Antenna System.



---

## Acknowledgement

---

I express my sincere gratitude to all the humans, who have guided and helped me, directly or indirectly during the time of my thesis. Without the kind support and guidance provided by those humans, it would not have been easy to complete the thesis successfully.

I express my gratitude towards my supervisor at Ericsson Raihan Rafique, for all the support and guidance throughout the thesis. Through continuous support, careful supervision of my work, he has always motivated me and uncomplainingly listened to my queries, stupid or otherwise. He always guided me towards the next milestone. I would also like to extend my thanks to Dimitar Nikolov, for understanding my perspective and helping me understand many difficult topics with his problem-solving approach and methodologies.

I would like to express my profound gratefulness towards Erik Larsson, Course Supervisor for Degree Project, EIT, Lund University, for his fruitful input and in-depth explanation of various issues that I encountered during my thesis. I thank him, for taking a keen interest in directing me all along, till the completion of my thesis.

I am really thankful to Himanshu Gaur at Ericsson for explaining several technical issues clearly. I am thankful to Åke Kristoffersson, Lab supervisor at Ericsson, for his guidance, time and providing me with all instrument that I required for the thesis work.

I want to thank Jacob Mannerstråle, manager at Ericsson, for granting me this valuable opportunity to do the thesis at Ericsson.

Finally, I express my gratitude to my family, who are far away, and their support, patience and motivation, has always boosted my morale & driven me to work incessantly.





## List of Acronyms

<b>AAS</b>	Advanced Antenna System
<b>ASIC</b>	Application Specific Integrated Circuit
<b>BiST</b>	Built-in Self-Test
<b>IoT</b>	Internet of Things
<b>LO</b>	Local Oscillator
<b>LTE</b>	Long Term Evolution
<b>MIMO</b>	Multiple Input Multiple Output
<b>MU-MIMO</b>	Multi-User MIMO
<b>PA</b>	Power Amplifier
<b>PSD</b>	Power Spectral Density
<b>RF</b>	Radio Frequency
<b>S-parameters</b>	Scattering Parameters
<b>SNR</b>	Signal to Noise Ratio
<b>VNA</b>	Vector Network Analyzer
<b>VNI</b>	Scattering Parameters



---

# Table of Contents

---

<b>1</b>	<b>Introduction</b>	<b>1</b>
1.1	Motivation . . . . .	1
1.2	Background . . . . .	2
1.3	Approach and Methodology . . . . .	5
1.4	Resources . . . . .	6
1.5	Outline . . . . .	6
<b>2</b>	<b>Related work</b>	<b>7</b>
2.1	Loopback testing . . . . .	7
2.2	Code-Modulated Embedded Test for Phased Arrays . . . . .	8
2.3	Built-In Self-Test of Transmitter IQ Mismatch . . . . .	9
<b>3</b>	<b>RF BiST Model</b>	<b>11</b>
3.1	The BiST Technique . . . . .	11
3.2	Measurement Setup . . . . .	13
3.3	PA Modeling . . . . .	15
3.4	Coupling coefficients . . . . .	17
<b>4</b>	<b>Experimental Results</b>	<b>19</b>
4.1	One Antenna Mathematical Model . . . . .	19
4.2	Results of the One Antenna Model . . . . .	19
4.3	2x1 Antenna Array Setup . . . . .	21
4.4	Results of the 2x1 Setup . . . . .	21
4.5	4x1 Antenna System Setup . . . . .	23
4.6	Results of the 4x1 Setup . . . . .	24
<b>5</b>	<b>Conclusion</b>	<b>27</b>
<b>6</b>	<b>Future Scope of Work</b>	<b>29</b>
	<b>References</b>	<b>31</b>



---

## List of Figures

---

1.1	Internet Of Things . . . . .	1
2.1	Loopback testing [11] . . . . .	7
2.2	Simplified block diagram of the phased-array (a) receiver and (b) transmitter outfitted with CoMET. Highlighted blocks indicate additional components unique to the proposed BiST architecture [7] . . . . .	9
2.3	Transceiver System Model with proposed BiST Circuitry . . . . .	10
3.1	Expected Output of the Self-Mixing Envelope Detector . . . . .	12
3.2	Flow Chart of the process of One Antenna model . . . . .	13
3.3	Flow Chart of the process of 2x1 Antenna model . . . . .	14
3.4	Measurement setup of the 2x1 Antenna model . . . . .	14
3.5	Flow Chart of the process of 4x1 Antenna model . . . . .	15
3.6	Outline of the Measurement Setup of PA Modeling . . . . .	16
3.7	S-Parameters Measurement setup for 1&2,3,4 . . . . .	17
4.1	Output of Mathematical Model with nominal impairments . . . . .	20
4.2	Measurement Setup of the 2x1 Antenna Array . . . . .	21
4.3	Output graph BiST Tx chain -1 . . . . .	22
4.4	Output graph BiST Tx chain -2 . . . . .	22
4.5	Simulation Setup of the 4x1 Antenna System . . . . .	24
4.6	Intermediate graphs of 4x1 Antenna Array setup . . . . .	25



---

## List of Tables

---

1.1	IQ Imbalances [14] . . . . .	4
3.1	S-Parameters for 4x1 Antenna Array . . . . .	18
4.1	IQ Impairments injected in One Antenna Model . . . . .	20
4.2	RMSE of IQ Impairments detection for One Antenna Model . . . . .	20
4.3	RMSE of the IQ Impairment detection for the 2x1 MIMO . . . . .	23
4.4	IQ Impairment detection for the 2x1 MIMO . . . . .	23
4.5	IQ Impairments injected in the 4x1 MIMO . . . . .	24
4.6	RMSE of IQ Impairments detection for 4x1 MIMO . . . . .	24





This chapter gives a concise overview of the distinct concepts being used in this thesis. It aims at providing an understanding of the thesis project.

## 1.1 Motivation

IoT is a network comprising uniquely distinctive everyday objects or devices equipped with a sensing system. IoT enables the objects, also called things, for sensing. This subsequently inter-operates and communicates with other objects for data exchange through an existing physical network infrastructure [19]. A typical representation of IoT is as shown in Figure 1.1. IoT incorporates multiple long-range, short-range, and personal area wireless networks and technologies into the designs of IoT applications [19]. As the playground of IoT is expanding, the number of IoT-enabled applications is rapidly growing, which results in a large scale growth of smart devices. IoT being applied in multiple service sectors constitutes this increase in the number of smart devices. Maintaining the high quality of service in these service sectors is very crucial. This has led to a remarkable increase in the demand for high data rates in wireless communication systems [19].



**Figure 1.1:** Internet Of Things

Shannon's theorem states that there is a maximum rate of transmitting data in a communications channel with a specified bandwidth in the presence of noise.

The theorem gives an upper bound to the capacity of a link, in bits per second per Hertz (b/s/Hz), as a function of the available bandwidth and the SNR ratio of the link [3]. The theorem can be stated as:

$$C = B * \log_2(1 + S/N)$$

where  $C$  is the achievable channel capacity,  $B$  is the channel bandwidth,  $S$  is the average signal power and  $N$  is the average noise power. Given a channel with particular bandwidth and noise characteristics, Shannon showed how to calculate the maximum rate at which data can be sent over the channel with zero error. This upper limit is often referred to as the Shannon limit [3].

To achieve high data rates, the modern wireless communication systems cannot only bank on increasing the bandwidth, as the currently used frequency spectrum is jam-packed. In this regard, the amelioration of antenna systems plays a major role in the current modern wireless communication systems. AAS, i.e MIMO, massive MIMO, Multi User MIMO (MU-MIMO), lead to considerable improvement in the modern wireless communication systems, by increasing not only the data rate but also spectrum efficiency and the channel capacity [8].

## 1.2 Background

### 1.2.1 Advanced Antenna Systems

According to the Cisco Visual Networking Index (VNI), global mobile data traffic has grown about 63 % in 2016 alone [2]. The ever growing mobile communications data traffic has recently drawn increased attention to a large amount of under-utilized spectrum in the millimeter-wave (mmW) frequency bands. It has been identified as a potentially viable solution for achieving tens to hundreds of times more capacity compared to the current 4G cellular networks [16].

The race to search for innovative solutions to handle the ever growing data traffic enable the 5G era has recently begun worldwide. Modern wireless communication standards like LTE and future 5G will be the primary focus of implementing technology for IoT. We have, AAS like MU-MIMO in current LTE and WLAN (802.11ad). However, for the 5G technology, the scale of MU-MIMO will be much larger and deployment will also be more common. In the multi/user scenario the system utilizes multiple antennas and beamforming technique to transmit multiple user data streams in the downlink [16].

In general, AAS is a system using an antenna array conjointly with a processor to adjust the radiation pattern according to the requirements. In wireless applications, especially long-range communications, directivity or high gain in a particular direction is required. In such applications radiation due to a single antenna element is too wide. A narrow beamwidth is necessary to increment the gain towards the required direction. Multiple spatially separated antennas, placed in a certain geometrical configuration, with more than one radiating element makes an antenna array. To form the coveted beam in a particular direction, proper current excitation is to be applied, to each antenna element [20].

To have the desired beam pattern, array synthesis is necessary. For correct array synthesis, number of array elements, geometrical orientation of array, and

spacing between elements of the array is paramount. If the array is synthesized properly, several beams can be generated using the same sets of multiple antennas. In a synthesized array, we can use precoding during the signal processing to modify the phase and/or amplitude of the current excitations to control the radiation pattern [20].

An antenna array is a set of  $N$  spatially separated antennas. The number of antennas in an array can be as small as 2, or as large as several thousand. In general, the performance of an antenna array, irrespective of the application, increases with the number of antennas (elements) in the array; the drawback of course is the increased cost, size, and complexity [1].

By manipulating amplitude and phase of the signals coming from each antenna element, the direction and shape of the signal beam from the multiple antenna system can be controlled. Thus, when signals of each element added, either constructively or destructively with the signals of the other elements, they form the desired beam. This technique is called Beamforming [10].

When the phase of the array is adjusted electronically, it is called analog Beamforming [15]. On the other hand, when precoding is used in signal processing at baseband to form the beam without steering actual beams into the channel, it is called digital Beamforming [17].

## 1.2.2 Mutual Coupling

Mutual coupling is a relatively general concept that may be understood in different ways. The most general definition of mutual coupling probably corresponds to the process through which the properties of a given radiator - mainly its input impedance & radiation pattern - are modified when another object is brought in the near field of the radiator. A possible interpretation of mutual coupling between several antennas is that the supporting element (the circuit to which the antenna is connected, the body of a person wearing the antenna, for instance) is part of the antenna, which therefore has other radiation properties than the isolated antenna [9].

It is difficult to say which is the minimal distance from which mutual coupling becomes negligible. In general, one will assume distances comparable to the wavelength [5].

Mutual coupling between antenna elements of an antenna array can be defined as the energy absorbed by one antenna's receiver when another nearby antenna is operating. This implies that mutual coupling is typically undesirable energy that should be radiated away is absorbed by a nearby antenna - in most of the usual cases it is detrimental to the antenna operation, although there are some examples in which its presence can be beneficial [9].

Basically, mutual coupling occurs due to the change of the electric current distribution on the antenna. When an object or another antenna is brought in the near field of a given radiator antenna, the changes are as following: [9]

- Radiator antenna can absorb a fraction of the radiated power by other antenna and input impedance is modified.
- Radiation pattern are modified.

Mutual coupling can be quantified by measuring the antenna isolation. Antenna to antenna isolation is a measure of how tightly coupled antennas are. The method of measuring isolation between 2 antennas is typically done by connecting both antennas to a Vector Network Analyzer(VNA), and measuring S12 (the transmission coefficient) [1].

Mutual coupling is the phenomenon which leads to crosstalk between antenna elements of the antenna array, which is undesirable and an unwanted effect. When designing a multi-antenna system, these crosstalk effects need to be considered in defining the system model [6].

### 1.2.3 IQ Imbalances

Vast majority of today's receivers are based on the traditional superheterodyne principle. In modern communication networks, more and more analog components are replaced by digital building blocks. This leads to less circuitry effort (chip size, power consumption, etc.) in the analog domain, but additional digital signal processing is required in order to remove spurious effects of the sub-optimum analog front-end [12].

A certain type of analog signal distortions, i.e. the in-phase (I) and quadrature-phase(Q) imbalances can severely damage the performance of the RF transceivers. In reality, there is always some imbalance in the analog front-end between the I and Q branch amplitudes and phases. This is mainly due to finite tolerances of capacitor and resistor values used to implement the analog components [21]. These errors can take place due to the Local Oscillator (LO) quadrature conversion. Although a perfectly balanced quadrature downconversion corresponds to a pure frequency translation, the imbalances introduce a frequency translation that results in a mixture of the image and the desired signals[21].

We conclude that these unwanted effects occur mainly due to amplitude- and phase-impairments between the local oscillator paths, due to mismatches & dc offset between the respective IQ-branches.

IQ imbalances are one of the most detrimental imperfections in transmitter performance. They can happen in the transmitter side or in the receiver side [14].

As a part of this thesis we only refer to the imbalances of the transmitter. Throughout this thesis, IQ imbalances in general, will refer to the following:

- Gain Mismatch : I and Q branches having a gain difference.
- Phase Mismatch : I and Q branches having a different phase difference.
- DC Offsets for both I and Q branches.

**Table 1.1:** IQ Imbalances [14]

Variable Name	Symbol
Gain Mismatch	$g_{tx}$
Phase Mismatch	$\varphi_{tx}$
TX DC Offsets	$DC_{I_{tx}} \& DC_{Q_{tx}}$

### 1.2.4 Digital BiST vs RF BiST

Testing a circuit requires the application of a test stimulus and the comparison of the actual circuit response with the correct response. Several techniques have been proposed for reducing the complexity of external testing by moving some or all of the tester functions onto the chip itself or onto the board on which the chips are mounted [13].

Any test method must consist of:

- a strategy for generating the inputs to be applied,
- a strategy for evaluating the output responses, and
- the implementation mechanisms.

The inclusion of on-chip circuitry for testing is called BiST. It is intended to reduce turnaround time to generate test patterns, the time taken to apply the test patterns, and the computation time, as well as reduce the cost of the testing solution [13].

Generally, the Digital BiST tells us where the fault in the system or the circuit is and we cannot do anything to fix it as a part of the BiST circuitry. It's not functionality of the Digital BiST.

RF Devices generally, work within a defined set of RF Parameters and these parameters are subject to corruption over time. They often deviate from the initially defined set and completely and/or partially change, due to the general wearing of the RF instrumentation, over the time. Unlike the Digital BiST, RF BiST would detect this degradation of the RF Parameters. A few of the RF Parameters can be fixed/corrected or digital amenable so that we can compensate for this degradation over time.

## 1.3 Approach and Methodology

Lets discuss the approach followed in detecting the IQ imbalances considering the crosstalk effects for the AAS.

- There are many techniques of RF BiST, but the most suitable one for detecting IQ imbalances is called Self-Mixing Envelope Detector method. A detailed description of this method is given in [14]. This BiST Technique is used in this thesis.
- A model of the IQ transmission chain, including the BiST circuitry (Self-Mixing), is implemented in Matlab and various simulations are conducted to evaluate the performance of the model.
- PA, crucial part of the IQ chain, is modelled using the Volterra series method of non-linear modeling. Coupling between different antenna elements is also modelled and coupling coefficients are extracted using a Vector Network analyser (VNA).
- Volterra series is used for modeling non-linearity of the PA. Two methods are available - Memory Polynomial(MP) and Generalised Memory Polynomial

(GMP) [6]. In this thesis, we have used a GMP to model the non-linearities of the PA.

- Mutual coupling between antenna elements occurs in multiple antenna systems and has significant effect on the signals being transmitted. We extract the coupling coefficients of the whole system (IQ Chain, upto the antenna, including the PA), by modelling the coupling, with the use of couplers and a VNA.
- Finally, designing the input signals and using the very near to reality models of the PA and the coupling coefficients and the BiST circuitry according to the paper [14], we built a mathematical model in Matlab and conducted simulations, to evaluate the whose results are tabulated in chapter 4. 3 cases have been considered - Single Antenna setup, 2x1 Antenna Array setup and 4x1 Antenna Array setup. Results of all three scenarios are in the Chapter 4.

## 1.4 Resources

This thesis work was done at Ericsson, Lund as a part of the Business Unit Radio Access Department. A workbench was provided in the Radio lab. In this thesis RF instruments like Digital Oscilloscope, Signal Generator, DC power source, RF switch, Signal Analyzer, Vector Network Analyzer (VNA) and other RF components, provided by Ericsson AB were employed. Along with the above components, a computer with a professional license enabled Matlab installed, was also available, in the Radio lab.

## 1.5 Outline

In this thesis, a number of RF BiST techniques have been studied as part of the literature review and one among them was chosen. A mathematical model of the chosen BiST Technique is built and scaled up to 2x1 and subsequently 4x1 Linear Antenna Array.

Chapter 1 discusses the motivation for this thesis, concepts required to understand this thesis work in brief and the problem in general. The rest of this report is organised as follows: Chapter 2 discusses related work in the field of research of the existing RF BiST Techniques, in brief and the chosen technique in a detailed fashion. The BiST technique, PA Modeling, Coupling coefficients extraction are described in Chapter 3. The mathematical model for a single antenna system, further scaling up the model to 2x1 Antenna system, their results and subsequently 4x1 Linear antenna array system is discussed, along with the results obtained are presented in chapter 4.

The final chapters 5 and 6 puts forward the conclusions of this thesis study and the future scope work that could be done further in this work.

Lets have a look at some related work in the field of interest, RF BiST. Various set of techniques being used in the RF self-testing domain were studied in detail and the most relevant ones are presented here in brief. For further reading into any of the techniques being discussed, the referenced papers are to be referred.

## 2.1 Loopback testing

BiST is important for more complex structures like complete front-ends, specifically RF front-end. This can be achieved in a couple of ways. The most obvious approach would be the separate testing of different single building blocks of the RF front-end. In this case every block corresponds to a device under test (DUT) and a special test signature will be formed according to the DUT's requirements. The advantage of this principle is a high test coverage due to special test stimulus that take into account all test conditions of the specific DUT. The processing of the DUT's signature response will need to be included as well. The main disadvantage of this method would be the high test overhead (Area required to implement this test strategy would be very high.) [11]

The second strategy is testing the whole transceiver front-end as a complete system. This is illustrated in the Figure 2.1. In this case the, DUT's structure corresponds to a series of building blocks of transmission chain, connected in a loop at the antennas. This principle is known from point-to-point radios as loopback technique [11].

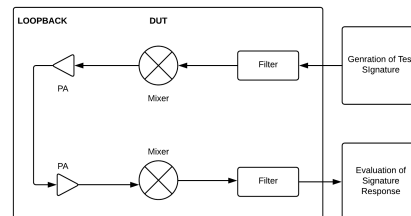


**Figure 2.1:** Loopback testing [11]

The main advantage of this loopback technique, compared to block testing



discussed earlier, is the low effort involved. The smaller test overhead is due to the technique not depending on the architecture and the technology of the DUT.

There are also disadvantages of this principle. Mainly, the test coverage is lower due to the fact, that the complete transceiver is tested as a whole. It could be possible to not detect bad spectral properties of the transmitted signal due to the masking by the receiver's selectivity [11].

## 2.2 Code-Modulated Embedded Test for Phased Arrays

RF and mm-wave BiSTs for Phased Antenna Arrays have been the subject of multiple investigations. First, a simple scalar approach is to use multiple power detectors distributed across the array. This method is simple and allows us to use simple non-coherent detectors to be used, but not only it doesn't allow us to measure the phase information but also would require us to first calibrate each individual detector across the array. Another approach would be to employ on-chip RF test distribution networks. This vector technique would allow the required measurement to be performed and also provide a way to obtain aggregate array responses on chip. But to obtain each elemental response, all other elements must be disabled, potentially changing the response of that individual element under test [7].

The authors of [7] propose a technique that employs code modulation for parallel in situ measurements of each element and a built-in distribution network to allow injection or extraction of RF/mm-wave test signals. The use of orthogonal code products (OCPs) where the product of any two codes is another specific code, is unique to their approach of BiST for Phased Arrays.

This paper [7], describes a free-space vector measurement technique for phased arrays that allows parallel extraction of each element's response and relies on code modulations and coherent receivers. In the approach proposed in [7], each phase-shifting element within a packaged antenna array is modulated using orthogonal codes.

For a transmitter array, signals are combined in space and then a coherent receiver placed in the far field downconverts the aggregate signal. For a receiver array, the setup is reversed, with a radiating source in the far field and then aggregation of code-modulated test signals occurring within the receiver under test. Each elemental vector response can be obtained through correlation of the received signal with the original code.

The aggregated test response is then down converted from radio-frequency or millimeter-wave (mm-Wave) frequencies by employing a direct (power) detector, resulting in a baseband interference signal composed of code-modulated complex cross correlations between all elemental signals. Use of the OCPs, allows each cross correlation to be extracted from the interference signal, and then the full set of cross correlations can be used to obtain amplitude and phase data of each element.

The authors refer to the proposed BiST solution as code-modulated embedded test (CoMET) and they refer to this measurement technique as code-modulated interferometry (CMI). The CoMET architecture to achieve this is shown in Figure

2.2 for both receive (Rx) and transmit (Tx) phased arrays.

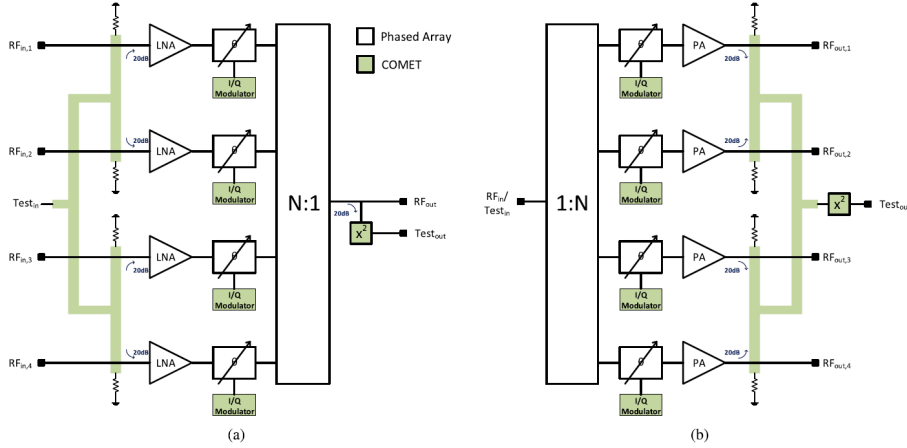


**Figure 2.2:** Simplified block diagram of the phased-array (a) receiver and (b) transmitter outfitted with CoMET. Highlighted blocks indicate additional components unique to the proposed BiST architecture [7]

The conclusion of that paper was that, the authors fabricated a four element 60-GHz phased-array receiver front end that includes this code-modulated embedded test (CoMET) infrastructure in BiCMOS technology. The BiST overhead is less than 2 % of the total die area. Comparisons between the proposed BiST technique and measurements using a vector network analyzer show that CoMET can be used to extract amplitude with 1 dB accuracy and phase with four degree accuracy. Furthermore, measurements confirm that CoMET can be used to extract the phase-step response of each element in parallel across all settings as well as phase offset introduced by the built-in test network [7].

### 2.3 Built-In Self-Test of Transmitter IQ Mismatch

Increasing circuit complexity and process variations drive the push toward including more on-chip structures to enable built-in characterization and calibration of radio frequency (RF) devices. Built-in self-test (BiST) for transmitters is a desirable choice since it eliminates the reliance on expensive instrumentation to perform radio-frequency signal analysis.

Existing on-chip resources, such as power or envelope detectors or small additional circuitry, can be used for BiST purposes. Due to limited bandwidth, measurement of complex specifications, such as In-phase and Quadrature (IQ) imbalances is challenging. Since IQ imbalances are most amenable for digital compensation, their characterization and monitoring are desirable. In this paper, the authors propose a multistep BiST technique for transmitter IQ imbalance and nonlinearity using a Self-Mixing Envelope Detector[21].

The authors derive analytical expressions for the output signal in linear and nonlinear modes. Using linear mode expression, they devise test signals to isolate the effects of gain and phase imbalances, dc offsets, and time skews from other parameters of the system in low-power mode.

In this thesis the IQ imbalances has been characterized using the Self-Mixing Envelope detector method described by the authors in [14]. We will go in detail about this in the following Section 2.3.1.

### 2.3.1 Defining IQ Mismatch and Self-Mixing Envelope Detector

System-level impairments and nonlinearity can severely damage the performance of the RF transceivers. IQ imbalance parameters impact the linear response of the circuit. To model, analyze, and compute the IQ imbalances, we derive a linear model of the overall path, including the envelope detector. IQ imbalances are one of the most detrimental imperfections in transmitter performance [14]. These IQ imbalances occur due to

IQ imbalances are defined and explained in detail in Section 1.2.3. Refer Table 1.1 for the definitions of the various IQ imbalances.

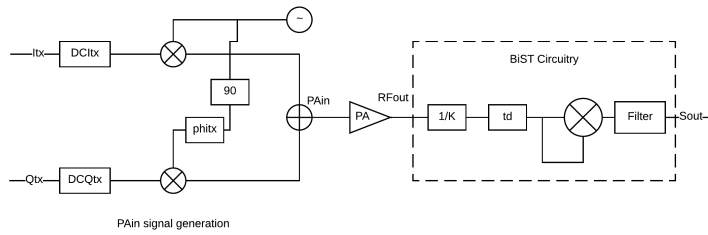


**Figure 2.3:** Transceiver System Model with proposed BiST Circuitry

In general, in RF BiST techniques, the high-frequency circuit response is converted into a low-frequency form, which is easier to analyze on-chip. The conversion needs to carry all the information pertaining to the desired parameters. For this purpose, the authors propose to use a self-mixing envelope detector, as shown in the Figure 2.3. The self-mixing envelope detector, as the name suggests, is a mixer whose local oscillator frequency is connected to the input itself - basically mixing the signal with itself [14].

In this chapter discuss in the approach and methodology described in Section 1.3. We describe the equations used in detecting the IQ imbalances present in the system and the expected output of the BiST circuitry. Measurement setup for all the three investigated cases is explained in detail. The modeling procedure for the PA and the extraction of the coupling coefficients in order to model the crosstalk effects of the AAS is also discussed in this chapter.

### 3.1 The BiST Technique

RF BiST technique described in [14], will be used in this thesis. Considering the Linear Model:

As the effect of nonlinearity depends on the power of input signal, we can make the DUT to operate in its linear range by limiting the input power below the 1-dB compression point. Operating in this range makes it easier to measure the linear IQ imbalance impairments with simple mathematical calculations.

The goal of this thesis is to detect these IQ parameters using simple calculations. The effect of the impairments can be observed at the output signal, these effects are added in the overall signal and separation of these parameters is not straightforward, especially in the presence of nonlinearity in the path. So, we need to devise a test signal which should help us to separate out each of these terms [14].

A sinusoidal test signal with two different frequencies is used for I and Q arms. Substituting the designed test signal into (3) and simplifying the result shows that there are seven frequency components in the BiST output signal in linear mode. This is illustrated in the Figure 3.1.

If  $\omega_1$  and  $\omega_2$  are the test signal frequencies on I and Q arms, the output signal includes dc,  $\omega_1$ ,  $\omega_2$ ,  $\omega_1 + \omega_2$ ,  $\omega_2 - \omega_1$ ,  $2\omega_1$ , and  $2\omega_2$  frequency components.

Due to the separation of the effect of different nonidealities on different frequency locations, one can use the amplitude of the frequency terms to compute these impairments and solve for them mathematically. Equations described below shows the amplitude expression for each of the frequency locations, while A is the amplitude of the input signal on both arms.

Computation of Gain, Phase Mismatch, and DC Offsets: [14]

With the above input signal, in the linear mode, one can observe seven frequency locations to analyze, as shown in the Figure 3.1. One can see that we also have five unknowns -  $G/K$ ,  $gtx$ ,  $\phi_{tx}$ ,  $DC_{Itx}$ , and  $DC_{Qtx}$  [14].

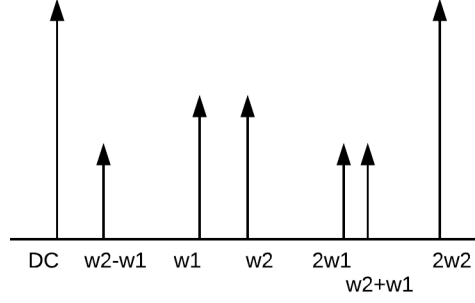


**Figure 3.1:** Expected Output of the Self-Mixing Envelope Detector

After extracting the amplitudes of the seven frequency locations from the frequency spectrum, one can use the following equations [14] to extract the five unknowns.

$$\frac{G}{K} = 2 * \sqrt{\frac{A_{2w_1}}{A^2}} \quad (3.1)$$

where,  $A_{2w_1}$  is the amplitude of the frequency location  $2w_1$ .

$$gtx = 2 * \sqrt{\frac{A_{2w_2}}{A^2 \left(\frac{G}{K}\right)^2}} - 1 \quad (3.2)$$

+ where,  $A_{2w_2}$  is the amplitude of the frequency location  $2w_2$ .

$$\phi_{tx} = \sin^{-1} \left( \frac{2A_{w_1-w_2}}{A^2 \left(\frac{G}{K}\right)^2 (1 + gtx)} \right) \quad (3.3)$$

where,  $A_{w_1-w_2}$  is the amplitude of the frequency location  $(w_1-w_2)$ .

$$DC_{Itx} = \frac{A_{w_1}(1 + gtx) + A_{w_2} \sin(\phi_{tx})}{A \left(\frac{G}{K}\right)^2 (1 + gtx) \cos^2(\phi_{tx})} \quad (3.4)$$

where,  $A_{w_1}, A_{w_2}$  is the amplitude of the frequency location  $w_1$  and  $w_2$  respectively.

$$DC_{Qtx} = \frac{A_{w_2} + A_{w_1}(1 + gtx) \sin(\phi_{tx})}{A \left(\frac{G}{K}\right)^2 (1 + gtx)^2 \cos^2(\phi_{tx})} \quad (3.5)$$

where,  $A_{w_1}, A_{w_2}$  is the amplitude of the frequency location  $w_1$  and  $w_2$  respectively.

In the equations described above, we obtain the five unknowns  $G/K$ ,  $gtx$ ,  $\phi_{tx}$ ,  $DC_{Itx}$ , and  $DC_{Qtx}$ . These equations are valid in both linear and non-linear cases.

## 3.2 Measurement Setup

The measurement setup used in this thesis is described in this section. We will be going through 3 cases in this section - 1 Antenna model, 2x1 Linear Antenna Array, and 4x1 Antenna Array. The One Antenna model and 4x1 Antenna Array model is simulated entirely in Matlab and the 2x1 Antenna Array model is implemented partly using real RF equipment & partly in Matlab.

The case of a single antenna model accounts for a single transmission chain which is illustrated in the Figure 2.3. A flow chart explaining the methodology followed is given in the Figure 3.2. The IQ signal with the impairments, namely PAin is generated via the Vector Signal generator (VSG: Agilent N5182A MXG). The frequencies chosen for I and Q are 4MHz and 5MHz respectively. This IQ signal is fed into the PA and the output is recorded in the spectrum analyzer (Spectrum analyzer details here). Now this recorded output is now fed into MATLAB program that mimics the Self-Mixing Envelope Detector, which is the proposed BiST Circuitry in [14].

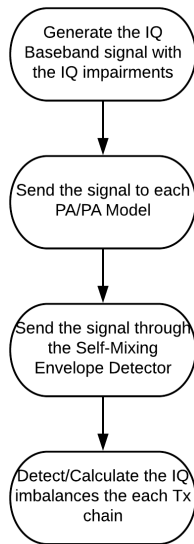


**Figure 3.2:** Flow Chart of the process of One Antenna model

The flow chart in the Figure 3.3 explains the process for the case of the 2x1 Antenna Model. The IQ signals with the impairments, are generated via the PXIe Vector Signal generator. The frequencies chosen for I and Q are same as before. These IQ signals are fed into each PA and then each output is passed through a directional coupler. These directional couplers are utilized to implement the cross coupling. This cross coupling is then varied with the use of different couplers or adding attenuators to the signal path. At the output of the directional couplers, an attenuator is purposefully added to minimize the reflected signal. Both the signal from each Tx chain is recorded simultaneously using the RF Switch and the spectrum analyzer. This recorded output is then passed through the Self-Mixing Envelope Detector. Figure 3.4 represents the block diagram of the Measurement

setup of the 2x1 Antenna Model system. Full Measurement Setup is shown in the experimental results chapter of this thesis.

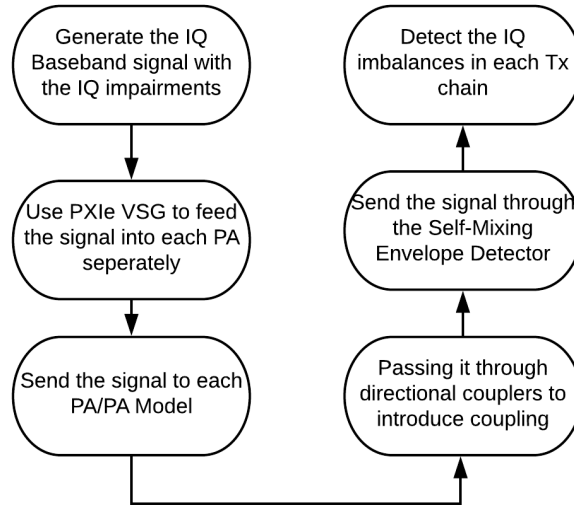


**Figure 3.3:** Flow Chart of the process of 2x1 Antenna model

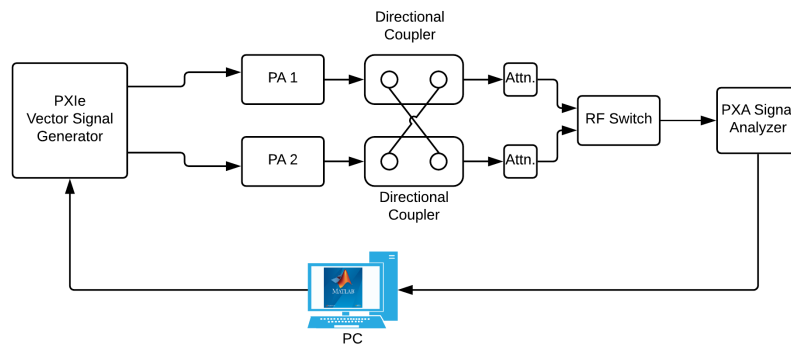


**Figure 3.4:** Measurement setup of the 2x1 Antenna model

The flow chart in the Figure 3.5 explains the process for the case of the 4x1 Antenna Model. A system level simulation is conducted using Matlab. The IQ signals with the impairments are generated. The frequencies chosen for I and Q are, once again, same as before. These IQ signals are fed into each PA model and then each output is passed through Self-Mixing Envelope Detector. A system level simulation is carried out in Matlab.

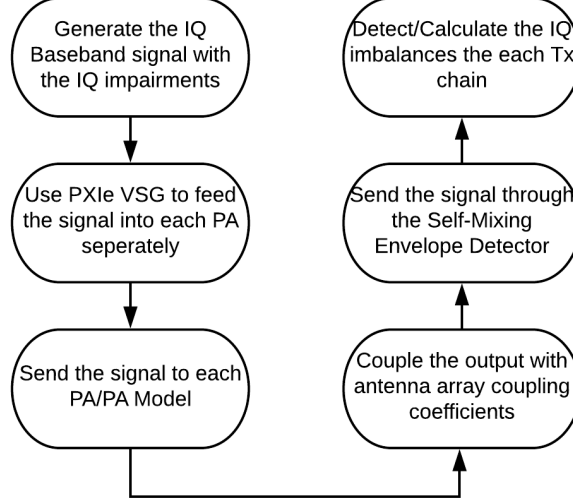


**Figure 3.5:** Flow Chart of the process of 4x1 Antenna model

### 3.3 PA Modeling

An overview of the PA Modeling is discussed in this chapter. To emulate the physical power amplifiers in a simulation model, mathematical models of power amplifiers used in the measurement setup are required. Since an ideal tool, for the system level simulation is required, for this reason, the behavioral modeling method is chosen here.

Treating the PA as a black box and relying on the observation of the input and output of the PA. The aim here is to build a model as close as to the physical PA, which is tuned by a mathematical expression, to match the output of the model with the output of the PA, when subjected to the same input signals.

A memory polynomial expression derived from the Volterra series models, is used to model the nonlinear relationship between input and output signals. Model Accuracy, computational complexity, the model extraction technique are the main criteria based on which this method was selected. The Volterra Model [4] [18] provides a general way to model a nonlinear system with memory, a combination of linear convolution and nonlinear power series. It is considered to be an extension of Taylor series. In this model the relationship between input and output signals is:

$$y(n) = \sum_{p=1}^P \sum_{i_1=0}^M \dots \sum_{i_p=0}^M h_p(i_1, \dots, i_p) \prod_{j=1}^p x(n - i_j) [18] \quad (3.6)$$

where  $x(n)$  and  $y(n)$  are the input and output signals.  $h_p(i_1, \dots, i_p)$  are the coefficients of the Volterra models. These are often referred as Volterra Kernels



[18] [6].  $P$  is the non-linearity order of the model and  $M$  is the memory depth.

Memory Polynomial (MP) model is widely known behavioral model based on reduction of Volterra Series model. It is a reasonable compromise on model accuracy and computational complexity. In this model only the diagonal elements are kept. Equation 3.7 gives the output of this model:

$$y_{MP}(n) = \sum_{k=0}^{K-1} \sum_{m=0}^{M-1} C_{km} V(n-m) |V(n-m)|^k [6] \quad (3.7)$$

where  $V(n)$  and  $y_{MP}(n)$  are the input and output signals,  $K$  is the non-linear order,  $M$  is the memory depth and  $C_{km}$  are the model coefficients. The memory polynomial model is a simplified case of Volterra model. A generalized form of the  $k_{th}$  memory polynomial in the Equation 3.7 can be written by inserting a local delay of  $m$  samples between the signal and its exponential parts. This delay could be of both different time shift (leading/lagging). This is called the Generalized Memory Polynomial Model (GMP). Equation 3.8 represents the GMP model:

$$\begin{aligned} y_{GMP}(n) = & \sum_{k=0}^{K_a-1} \sum_{l=0}^{L_a-1} a_{kl} V(n-l) |V(n-l)|^k \\ & + \sum_{k=1}^{K_b-1} \sum_{l=0}^{L_b-1} \sum_{m=1}^{M_b} b_{klm} V(n-l) |V(n-l-m)|^k \\ & + \sum_{k=1}^{K_c-1} \sum_{l=0}^{L_c-1} \sum_{m=1}^{M_c} c_{klm} V(n-l) |V(n-l+m)|^k \end{aligned} \quad (3.8)$$

where the first part is the same as the memory polynomial model [18], the other two terms are the cross memory with both positive and negative time shifts.  $M_a$  - memory depth,  $K_a$ -nonlinearity order and  $a_{mk}$  - model parameters or kernels.  $M_b, K_b, L_b$  and  $b_{mlk}$ , are the terms for lagging time shift of memory depth, nonlinearity order, model parameters or kernels respectively, whereas  $M_c, K_c, L_c$  and  $c_{mlk}$  are the terms for leading time shift of memory depth, nonlinearity order, model parameters or kernels respectively. The outline of the measurement setup used for PA Modelling is given in the Figure 3.6.

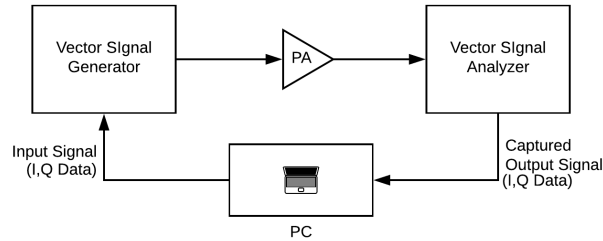


**Figure 3.6:** Outline of the Measurement Setup of PA Modeling

### 3.4 Coupling coefficients

Mutual Coupling between antenna is an electromagnetic phenomenon. It occurs due to the change of the electric current distribution on the antenna. Many methods to study the effects of the mutual coupling in array antennas have been proposed. As the radio transceivers' size is decreasing and small-size of the antenna arrays, the effect of mutual coupling is more important than ever. To understand the effects of the mutual coupling, scattering characteristics (S-parameters) between the antenna elements were measured using a Vector Network Analyzer (VNA).

In this thesis, coupling values of 4x1 uniform linear array were measured via a 4-port VNA. Modeling the crosstalk of the array, we measure the scattering characteristics also known as S-parameters. Since we are measuring the coupling of a 4x1 linear array, and a 4-port measurement is a very simple method to extract the coupling coefficients between the antenna array elements. We will have to do the measurement for 4 different cases. We couple the 1st Tx chain with the 2nd, 3rd and 4th Tx chain, as shown in the Figure 3.7. We then conduct the measurement, for coupling the 1st, 3rd and 4th Tx chain and the 2nd Tx chain. This process is done 4 times in total and we only collect the S12 parameters, that become our coupling coefficients.

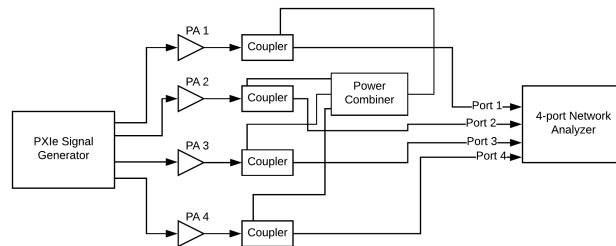


**Figure 3.7:** S-Parameters Measurement setup for 1&2,3,4

The coupler shown in the Figure 3.7 is Microlab CK-6 series. It is a 7dB directional coupler and has 3 ports. In the Figure 3.7, we are coupling 1st Tx chain with the 2nd, 3rd and 4th Tx chain, where we have flipped the coupler for the 1st Tx chain and use the coupler normally in the 2nd, 3rd and 4th Tx chains. We repeat this process four times and collected the coupling coefficients for each transmission chain. We use the coupling coefficients, extracted through the above method, in the 4x1 Antenna Array case, discussed in the previous section 3.2. For the carrier frequency 2.44 GHz, S-parameter data from VNA was processed through Matlab, and Table 3.1 gives us the S-parameters of the 4x1 Antenna Array.

**Table 3.1:** S-Parameters for 4x1 Antenna Array

Tx-1	Value (dB)	Tx-2	Value (dB)	Tx-3	Value (dB)	Tx-4	Value (dB)
S11	-4.2	S21	-41	S31	-41.9	S41	-39.5
S12	-40.25	S22	-5.45	S32	-40.9	S42	-40.6
S13	-45.82	S23	-45.3	S33	-5.35	S43	-44.19
S14	-40.9	S24	-34.2	S34	-45.85	S44	-4.36

---

## Experimental Results

---

Input signal with impairments is generated using Matlab. It is beneficial to use a high separation between the input frequencies of the signal tones [14]. Hence, we proceed with I and Q frequencies being 4MHz and 5MHz. Let us now dive into more detail about the measurement setups and results obtained. 2 transmission chain partly implemented using RF equipment and Matlab model and one transmission chain & 4 transmission chains models - using the PA Model and coupling model described in the section 3.3 and section 3.4, respectively were created.

- One Antenna Mathematical Model
- 2x1 Antenna Array Setup/ 2x1 MIMO Setup
- 4x1 Antenna Array Setup/ 4x1 MIMO Setup

### 4.1 One Antenna Mathematical Model

In this section we will be investigating the One Antenna Matlab Model in detail. This model is based on the Figure 2.3. We have designed an input signal with input power around -20dBm. Inout frquencies of the I and Q signal are kept as 4MHz and 5 MHz. The LO frequency is kept as 2.44GHz as the PA, from mini-circuits used in this thesis gives us a maximum gain at that particular frequency. IQ imbalances/impairments are added in this signal generation phase. We then passed this IQ signal through the GMP PA model. We have modeled this PA using the GMP PA modeling procedure described in the section 3.3.

The output of the PA Model is then fed into the BiST Circuitry part of the Matlab model and then further calculations are carried out. This enables us to detect the IQ impairments with low computational complexity. Table 4.1 gives us the injected IQ impairments added to the input signal. System level simulations are performed. I'll discuss the results obtained from these simulations in the following section.

### 4.2 Results of the One Antenna Model

The output graph shown in the Figure 4.1 is a power spectral density (PSD) plot of the output of the BiST circuitry matlab model. It is included here to showcase

**Table 4.1:** IQ Impairments injected in One Antenna Model

Parameter	Injection Limit
$DC_{I_{tx}}$	[0,30mV]
$DC_{Q_{tx}}$	[0,30mV]
Phase Mismatch	[0°,4°]
Gain Mismatch	[-2,3]

**Table 4.2:** RMSE of IQ Impairments detection for One Antenna Model

Parameter	RMSE%
$DC_{I_{tx}}$	3.2172
$DC_{Q_{tx}}$	9.2650
Phase Mismatch	3.7731
Gain Mismatch	3.5965

a mere sample of the outputs recorded during sweeping the injected impairments added to the input signal during the initial input generation phase. The graph in the Figure 4.1 refers to one particular case where the impairments added were: Gain mismatch = 1.5%, Phase mismatch = 2°,  $DC_{I_{tx}} = DC_{Q_{tx}} = 10\text{mV}$ . The wanted signal components, are 1, 4, 5, 8, 9, and 10MHz, which can be discerned in the Figure 4.1.

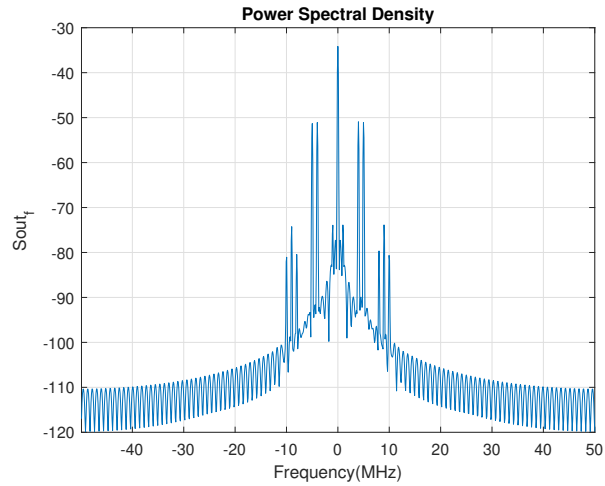
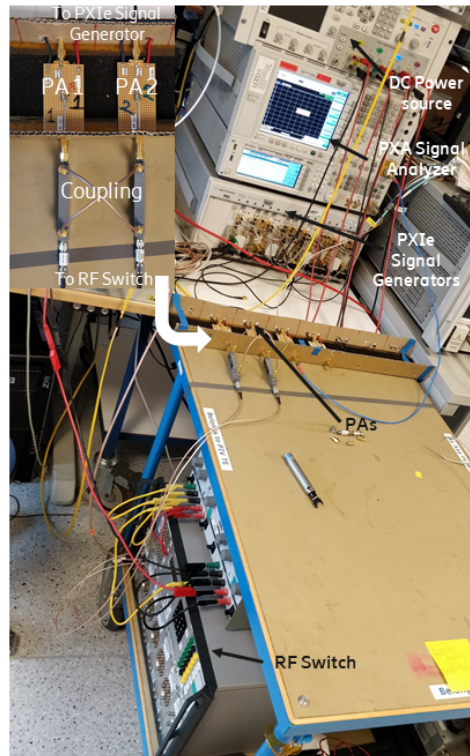
**Figure 4.1:** Output of Mathematical Model with nominal impairments

Table 4.2 shows the Root Mean Square Error (RMSE) of all the calculated IQ impairments. The results resonate with the results presented in [14], where the

BiST circuitry was originally proposed. This proves that the PA model and the Self-Mixing Envelope Detector method is working as intended.

### 4.3 2x1 Antenna Array Setup

Let us now investigate the 2x1 Antenna Array setup, also known as, 2x1 MIMO setup. One part of this setup is implemented using RF Equipment and the other part is implemented using Matlab. Input signals with I and Q frequencies being 4MHz and 5MHz, along with the impairments added to the signal in the generation phase, are sent using the PXIe Vector Signal Generator (M9018A) to the two PAs. After the outputs of the PAs are coupled, these signals are recorded via the PXA signal analyzer, through the RF switch and then passed through the Self-Mixing Envelope Detector Matlab program and IQ impairments are detected. This full Measurement Setup is shown in the Figure 4.2.



**Figure 4.2:** Measurement Setup of the 2x1 Antenna Array

### 4.4 Results of the 2x1 Setup

The output of the setup for 2x1 Antenna Array described in the Figure 4.2 after passing it through the BiST Circuitry implemented in Matlab is given in the Figure

4.3 & Figure 4.4, for the 1st Tx chain and 2nd Tx chain respectively. These are the power spectral density plots, and give us the frequency domain information of the output. When compared to 3.1, one can clearly match these peaks. The aspired signal components, in this case, are 1, 4, 5, 8, 9, and 10MHz, which can be discerned in both the figures.

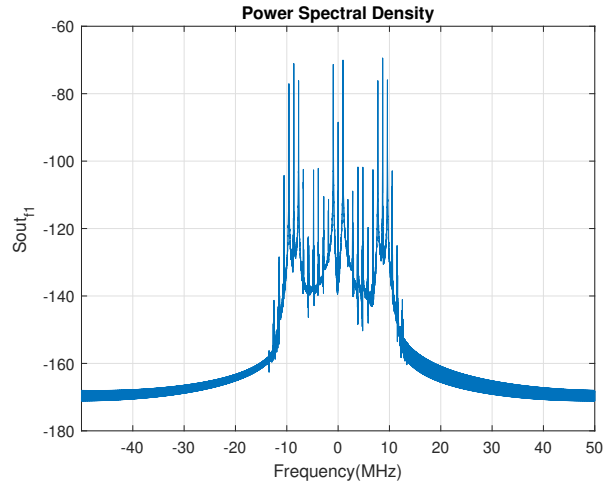


**Figure 4.3:** Output graph BiST Tx chain -1

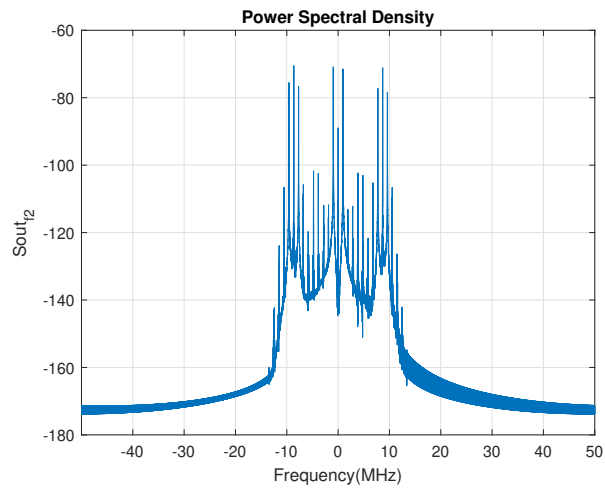


**Figure 4.4:** Output graph BiST Tx chain -2

Table 4.3 gives us the Root Mean Square Error (RMSE) of the BiST circuitry, Self-Mixing Envelope Detector to detect the IQ impairments injected in the input signal. In Table 4.3 RMSE % 1 - refers to the RMSE% of the Tx chain -1, and similarly RMSE% 2 refers to the Tx chain -2.

**Table 4.3:** RMSE of the IQ Impairment detection for the 2x1 MIMO

Parameter	RMSE%1	RMSE%2
$DC_{I_{tx}}$	0.7542	2.8939
$DC_{Q_{tx}}$	9.0570	8.5378
Phase Mismatch	8.6692	8.7779
Gain Mismatch	6.9847	7.2034

**Table 4.4:** IQ Impairment detection for the 2x1 MIMO

	Parameter	Actual	Computed	Error
Tx-1 chain	$DC_{I_{tx}}$	10mv	1.1mV	8.9mV
	$DC_{Q_{tx}}$	10mV	5.7mV	4.3mV
	$Phase_{MM}$	4°	4.56°	0.56°
	$Gain_{MM}$	10%	8.9%	1.1%
Tx-2 chain	$DC_{I_{tx}}$	10mv	4.1mV	5.9mV
	$DC_{Q_{tx}}$	10mV	4.6mV	5.4mV
	$Phase_{MM}$	4°	4.87°	0.87°
	$Gain_{MM}$	10%	7.7%	2.3%

Table 4.4 shows the measurement results of both the Tx chains. The DC offsets are measured upto 10mV error. Gain Mismatch can be measured upto 2.3%, whereas the Phase Mismatch upto 0.87°. The measurements are slightly higher, because of the higher noise in the system, limitations of the equipment and deviations of the potentially unmodelled behaviors. However, the errors are very close to the results in [14] even though the system used in [14] did not have the any coupling whatsoever and had only one Tx-chain.

## 4.5 4x1 Antenna System Setup

In this case, analysis the 4 transmission chain model, was created in Matlab. We used the GMP PA model, coupling coefficients described in the Table 3.1. Figure 4.5 shows the simulation setup of the 4x1 Antenna Array. Input frequencies are again 4MHz and 5MHz.

These input signals are then passed through PA models, modelled using PA modeling process described in the Section 3.3, which is then matrix multiplied with the S-parameter matrix in the Table 3.1, giving us the coupled signals. This coupled output is now passed through the Self-Mixing Envelope Detector and the output, through the calculations now helps us detect the IQ impairments present in the system.

Table 4.5 gives us the injected IQ impairments into the system in the initial signal generation phase of the Matlab model.



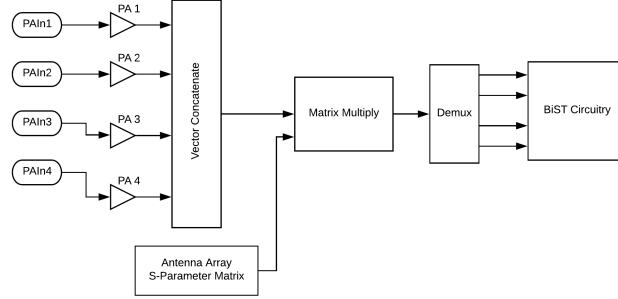


**Figure 4.5:** Simulation Setup of the 4x1 Antenna System

**Table 4.5:** IQ Impairments injected in the 4x1 MIMO

Parameter	Injection Limit
$DC_{Itx}$	[0,30mV]
$DC_{Qtx}$	[0,30mV]
Phase Mismatch	[0°,4°]
Gain Mismatch	[-2,3]

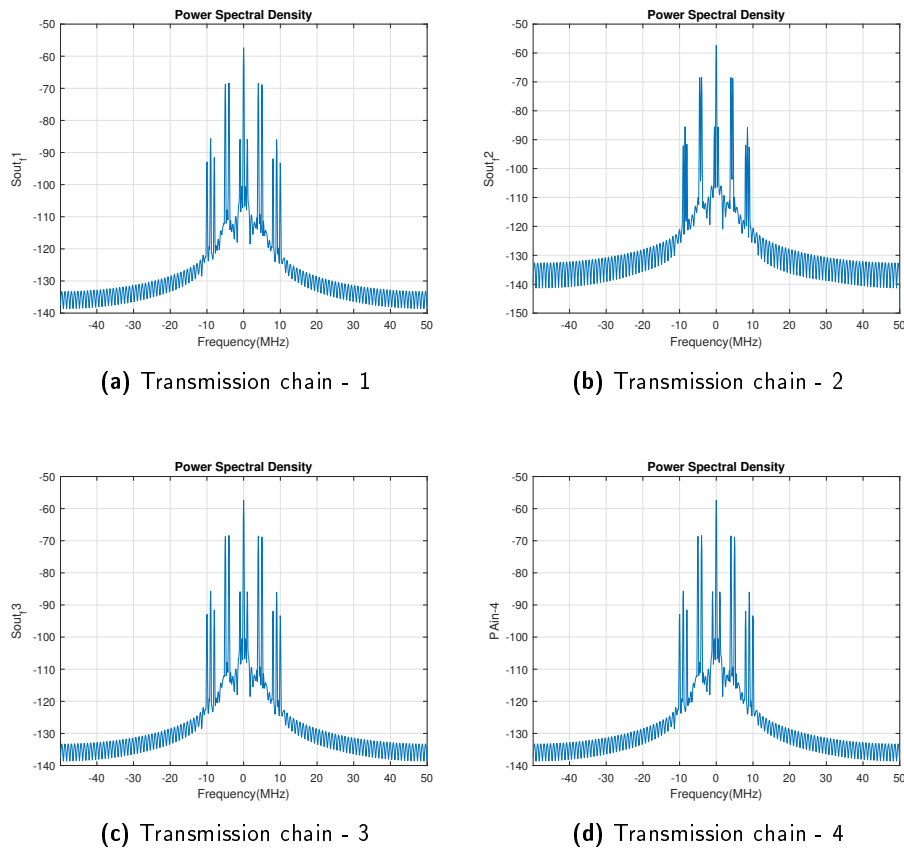
## 4.6 Results of the 4x1 Setup

Figure 4.6 shows the power spectral density of the outputs of the BiST circuitry for the 4x1 Antenna array setup. These figures are a representation of how the output will look like. These are a sample of the 100s of plots generated by the Matlab model as we are sweeping the IQ impairments, given in the Table 4.5. Figure 4.6a is the output of the transmission chain 1, Figure 4.6b is the output of the transmission chain 2, Figure 4.6c is the output of the transmission chain 3, and Figure 4.6d is the output of the transmission chain 4. These plots are used to get the frequency domain information required.

**Table 4.6:** RMSE of IQ Impairments detection for 4x1 MIMO

Parameter	RMSE%1	RMSE%2	RMSE%3	RMSE%4
$DC_{Itx}$	2.5274	9.7178	9.2316	3.1050
$DC_{Qtx}$	9.5157	3.2257	9.0323	8.4522
Phase Mismatch	0.6619	9.7708	9.1860	3.3248
Gain Mismatch	0.6617	9.7713	9.1860	3.3248

Table 4.6 gives us the Root Mean Square Error (RMSE) of the calculated IQ impairments using the Self-Mixing Envelope Detector method. This helps to detect the IQ impairments injected in the input signal. In Table 4.3 RMSE % 1 - refers to the RMSE % of the Tx chain -1, and RMSE % 2 refers to the RMSE % of the Tx chain -2, RMSE % 3 refers the Tx chain -3, RMSE % 4 the Tx chain 4. These results



**Figure 4.6:** Intermediate graphs of 4x1 Antenna Array setup

once again are very similar to the one antenna matlab model, confirming that this BiST circuitry, Self-Mixing Envelope Detector method enables us to detect the IQ imbalances to a certain accuracy, which is well within the acceptable range and with low computational complexity.



In this thesis work, we established a RF BiST solution for Advanced Antenna System with low computational complexity, which enables us to detect the IQ imbalances. After going through various existing BiST solution which were applied to various scenarios, during literature review, the BiST Technique proposed in [14] was chosen for further investigation and extending the application of the proposed Self-Mixing Envelope Detector from one transmission chain to multiple transmission chains (upto 4), referred to as Advanced Antenna Systems.

First, we built one antenna model, in Matlab, of the system analysed in the main reference paper [14]. This has helped me make sure that the PA model and the Self-Mixing Envelope Detector method is working as intended. RMSE calculations of the one antenna matlab model are given in the Table 4.2. These RMSE % results for all the IQ imbalances are  $<10\%$  which resonate with the findings presented in [14]. This confirms that matlab model mimics the proposed BiST circuitry and enables us to detect IQ imbalances with low computational complexity.

We then extended this method to a 2x1 Antenna array, also known as 2x1 MIMO. Now, in this case there are 2 transmission chains. This setup was partly implemented, using the RF equipment and partly using matlab. The measurement setup is shown in Figure 4.2 and in the Figure 3.4. The results are tabulated in the Table 4.4 of both transmission chains and Table 4.3 gives the RMSE% of both the transmission chains. Gain Mismatch can be measured upto 2.3%, whereas the Phase Mismatch upto  $0.87^\circ$ . DC offsets are measured upto 10mV error. The impact of the coupling was studied in detail in this case. The impact of considering these crosstalk effects was not found to be effecting the performance of the BiST circuitry.

Extending this BiST circuitry further to a 4x1 Antenna Array setup, which is also known as 4x1 MIMO. We used the same PA Model used in the one antenna matlab model, it is described in section 3.3 and the coupling is modeled using the coupling coefficients defined in the 3.4. Multiple system level simulations were performed and results were collected and tabulated. Table 4.6 gives the RMSE of all the 4 transmission chains. This confirms the results observed in the both the previous cases as well. Hence we conclude, that the proposed BiST circuitry - Self-Mixing Envelope Detector method, enables us to detect the IQ imbalances considering the crosstalk effects for the advanced antenna system.



---

## Future Scope of Work

---

The thesis work has fulfilled most of the intentions, but however, more work could be done when it comes to improving the design and different methods could be explored, to produce better results. Several challenges concerning restrictions with the setup used for the measurement, interfacing simulation design of the BiST circuitry can be approached in future work.

When it comes the existing design implemented in this thesis work, the entire system of 2x1 antenna array setup can be implemented using only the RF equipment and more accurate results can be obtained. Even the complete 4x1 antenna array setup can be implemented using RF equipment and those results can be compared to the simulated results obtained in this thesis. An Application Specific Integrated Chip (ASIC) could be designed from scratch. Also, processing time (delay) of the 2x1 antenna array setup varies with each iteration, particularly even more problematic if changes to the input signal was made or if one wishes to run a hundred thousand sample-based iteration, to obtain better results.

One can simply increase the number of transmission chains from 4, and check if the BiST Circuitry holds up. Measurement setup for much more accurate modeling of the crosstalk effects could be realized, which would further help us confirm the results. A much more accurate method to not only detect the IQ impairments of the system, but also pinpoint the exact transmission chain in which the IQ impairment is present could be explored. One can also improve the accuracy of the method, by using better hardware setup.

An ASIC for the Self-Mixing Envelope Detector could be implemented and used as a on-chip self test block. A better architecture design of this BiST Circuitry, with low-power, low-area design could be achieved and implemented. This architecture can be designed from transistor level design. This design could later be synthesized, and a tape out version of the design could be implemented and robustness of that ASIC could be tested out, to confirm the results obtained in this thesis.



---

## References

---

- [1] Antenna Arrays (Phased Arrays). Accessed: 2018-04-29.
- [2] Cisco Visual Networking Index: Global Mobile Data Traffic Forecast Update, 2016–2021 White Paper - Cisco.
- [3] Shannon Theorem. Accessed: 2018-11-01.
- [4] Sergio Benedetto, Ezio Biglieri, and Riccardo Daffara. Modeling and performance evaluation of nonlinear satellite links-a Volterra series approach. *IEEE Transactions on Aerospace and Electronic Systems*, (4):494–507, 1979.
- [5] Christophe Craeye, Belen Andrés García, Enrique García Muñoz, and Rémi Sarkis. An open-source code for the calculation of the effects of mutual coupling in arrays of wires and for the ASM-MBF method. *International Journal of Antennas and Propagation*, 2010, 2010.
- [6] Himanshu Gaur and Md Zahidul Islam Shahin. Efficient DPD Coefficient Extraction For Compensating Antenna Crosstalk And Mismatch Effects In Advanced Antenna System, 2018. Student Paper.
- [7] Kevin Greene, Vikas Chauhan, and Brian Floyd. Built-In Test of Phased Arrays Using Code-Modulated Interferometry. *IEEE Transactions on Microwave Theory and Techniques*, 66(5):2463–2479, 2018.
- [8] Andreas Hoglund, Xingqin Lin, Olof Liberg, Ali Behravan, Emre A Yavuz, Martin Van Der Zee, Yutao Sui, Tuomas Tirronen, Antti Ratilainen, and David Eriksson. Overview of 3GPP release 14 enhanced NB-IoT. *IEEE Network*, 31(6):16–22, 2017.
- [9] Hon Tat Hui, Marek E Bialkowski, and Hoi Shun Lui. Mutual coupling in antenna arrays. *International Journal of Antennas and Propagation*, 2010, 2010.
- [10] Sean Victor Hum. ECE422 - Radio and Microwave Wireless Systems.
- [11] Doris Lupea, Udo Pursche, and H-J Jentschel. RF-BIST: Loopback spectral signature analysis. In *Design, Automation and Test in Europe Conference and Exhibition, 2003*, pages 478–483. IEEE, 2003.



- 
- [12] M Mailand, R Richter, and H-J Jentschel. IQ-imbalance and its compensation for non-ideal analog receivers comprising frequency-selective components. *Advances in Radio Science*, 4(D. 1):189–195, 2006.
- [13] Edward J McCluskey. Built-in self-test techniques. *IEEE Design & Test of Computers*, 2(2):21–28, 1985.
- [14] Afsaneh Nassery, Srinath Byregowda, Sule Ozev, Marian Verhelst, and Mustapha Slamani. Built-in self-test of transmitter I/Q mismatch and nonlinearity using self-mixing envelope detector. *IEEE Transactions on Very Large Scale Integration (VLSI) Systems*, 23(2):331–341, 2015.
- [15] M Reil and G Loyd. Millimeter-wave beamforming: Antenna array design choices & characterization. *Rhode and Shwartz White Paper*, 2016.
- [16] Wonil Roh, Ji-Yun Seol, Jeongho Park, Byunghwan Lee, Jaekon Lee, Yungsoo Kim, Jaeweon Cho, Kyungwhoon Cheun, and Farshid Aryanfar. Millimeter-wave beamforming as an enabling technology for 5G cellular communications: Theoretical feasibility and prototype results. *IEEE communications magazine*, 52(2):106–113, 2014.
- [17] Adel AM Saleh. Frequency-independent and frequency-dependent nonlinear models of TWT amplifiers. *IEEE Transactions on communications*, 29(11):1715–1720, 1981.
- [18] Martin Schetzen. The Volterra and Wiener theories of nonlinear systems. 1980.
- [19] Sugam Sharma. Brief Summary on IoT. 2016.
- [20] MN Md Tan, SKA Rahim, MT Ali, and TA Rahman. Smart Antenna: Weight Calculation and Side-lobe Reduction by Unequal Spacing Technique. In *RF and Microwave Conference, 2008. RFM 2008. IEEE International*, pages 441–445. IEEE, 2008.
- [21] Mikko Valkama, Markku Renfors, and Visa Koivunen. Advanced methods for I/Q imbalance compensation in communication receivers. *IEEE Transactions on Signal Processing*, 49(10):2335–2344, 2001.



**LUND**  
UNIVERSITY

Series of Master's theses  
Department of Electrical and Information Technology  
LU/LTH-EIT 2018-675  
<http://www.eit.lth.se>